Electromagnetic-Thermal Analysis of Human Head Exposed to Cell Phones With the Consideration of Radiative Cooling

Huan Huan Zhang, *Member, IEEE*, Zhong Chao Lin, Wei E.I. Sha, *Senior Member, IEEE*, Wai Wa Choi, *Senior Member, IEEE*, Kam Weng Tam, *Senior Member, IEEE*, Daniel Garcia Donoro, and Guangming Shi, *Senior Member, IEEE*

***Abstract*—The influences of electromagnetic radiation from mobile phones on human health have aroused significant public concern. One of the most serious consequences is the increment of temperature of tissues and organs. Due to the specificity of the research object, numerical methods for electromagnetic and thermal analysis are usually adopted instead of trials. Most of the existing studies adopt a finite-difference time-domain method for electromagnetic and thermal simulation. Moreover, the radiative cooling phenomenon is neglected during the thermal simulation. In this letter, we utilized the finite-element method with tetrahedral elements to get a better modeling of the human head. Furthermore, the radiative cooling is also taken into account by using the radiation boundary condition. Numerical results validate the accuracy and capability of the proposed method.**

***Index Terms*—Convective cooling, finite-element method (FEM), radiative cooling, specific absorption rate (SAR), thermal simulation.**

I. Introduction

SINCE the invention of cell phones, it has become more and more indispensable in people's daily lives due to its mobility, versatility, convenience, and affordability. When a cell phone is in operation, it will transmit electromagnetic waves, and a substantial part of them will be absorbed by human bodies, especially human heads. The most immediate adverse effect is the increment of temperature of tissues and organs. It is reported that a small temperature increase in the brain of about 3.5 °C will lead to physiological damage [1]. Therefore, a thorough study of the thermal effects on the human head induced by the radiation of cell phones can provide guidelines for their design, manufacture, and usage, thus avoiding or reducing their influence on human health.

Due to the ethical consideration, experimental studies of electromagnetic and thermal effects on the human body are impractical. Thus, numerical methods including the method of moments (MOM) [2], [3], finite-difference time-domain (FDTD) method [4]–[8], and finite-element method (FEM) [9]–[11] are widely adopted. After making a thorough survey of current research, we found the following: 1) The MOM is not convenient to deal with highly inhomogeneous materials like human head. The FDTD method is the most popular numerical method for both electromagnetic and thermal simulation of the human body due to its simplicity and efficiency. However, orthogonal grids are adopted in conventional FDTD method, resulting in a degeneration of the geometrical information due to the staircase effect. The FEM with tetrahedral elements allows for conformal modeling of geometries with curved surfaces, resulting in better accuracy. 2) In most of the works, only electromagnetic simulation is involved to obtain the specific absorption rate (SAR) values of tissues, while the electromagnetic and thermal cosimulation is less studied. Actually, the temperature increments in tissues are not directly proportional to the local SAR values [4]. Therefore, it is necessary to conduct electromagnetic and thermal cosimulation. 3) In nearly all of the studies on thermal simulation of the human body, only convective boundary condition is imposed at the interface of skin and air, while the radiative cooling phenomenon is ignored. Actually, all objects that are above absolute zero temperature radiate electromagnetic waves to surroundings. It is said that 60% of total heat loss of a nude person sitting at normal room temperature is by radiation [1]. Thus, it is unreasonable to neglect the radiative cooling of skin in the thermal simulation of the human body.

Based on the above considerations, we propose to use the FEM for electromagnetic and thermal cosimulation. Moreover, both the convective and radiative boundary conditions are adopted during thermal simulation to get a more accurate temperature distribution of the human head.

Manuscript received May 15, 2018; revised June 17, 2018; accepted July 11, 2018. Date of publication July 16, 2018; date of current version August 31, 2018. This work was supported in part by the National Key R&D Program of China under Grant 2016YFE0121600, in part by the Joint Research Project of the Ministry of Science and Technology of PRC and the Macao Science and Technology Development Fund under Grant 014/2015/AMJ, in part by the National Natural Science Foundation of China under Grant 61701376; in part by the General Financial Grant from the China Postdoctoral Science Foundation under Grant 2017M613071 and Grant 2018T111016, and in part by the Open Project Foundation of the State Key Laboratory of Millimeter Waves under Grant K201808. *(Corresponding author: Zhong Chao Lin.)*

H. H. Zhang is with the School of Electronic Engineering, Xidian University, Xi'an 710071, China, and also with the Faculty of Science and Technology, University of Macau, Macau (e-mail: hhzhang@xidian.edu.cn).

Z. C. Lin, D. G. Donoro, and G. Shi are with the School of Electronic Engineering, Xidian University, Xi'an 710071, China (e-mail: zclin@xidian.edu.cn; daniel@xidian.edu.cn; gmshi@xidian.edu.cn).

W. E. I. Sha is with the College of Information and Electronic Engineering, Zhejiang University, Hangzhou 310058, China (e-mail: weisha@zju.edu.cn).

W. W. Choi and K. W. Tam are with the Faculty of Science and Technology, University of Macau, Macau (e-mail: welsyc@umac.mo; kentam@umac.mo).

Digital Object Identifier 10.1109/LAWP.2018.2856365

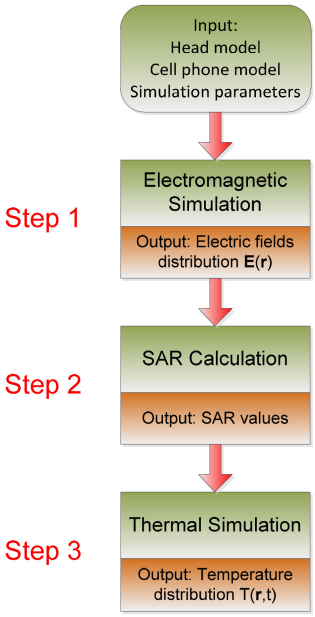

Fig. 1. Flow diagram for the electromagnetic-thermal analysis of human head exposed to cell phones.

II. Principle and Formula

As shown in Fig. 1, there are mainly three steps for an electromagnetic-thermal analysis of the human head exposed to cell phones. First, the electromagnetic simulation is performed to obtain the electric field distribution $\mathbf{E}(\mathbf{r})$ of the head model. The numerical method for electromagnetic simulation adopted in this letter is the finite element-iterative integral equation evaluation (FE-IIEE) method [12], [13]. The FE-IIEE method provides an arbitrarily accurate radiation boundary condition for the FEM by means of an integral equation method. A detailed introduction of the FE-IIEE method is out of the scope of this letter; the readers can refer to [12] and [13] for further information of this method.

The energy of the electromagnetic waves radiated from a cell phone will be absorbed by the human head. The SAR value is utilized to measure the rate of electromagnetic energy absorbed by the biological tissues. It is defined as the power absorbed per mass of tissue. It can be calculated as

$$\mathrm{SAR} = \frac{\sigma |\mathbf{E}(\mathbf{r})|^2}{\rho} \tag{1}$$

where σ refers to the local conductivity and ρ represents the local density.

After we get the SAR distribution of the human head model, thermal simulation can be carried out to acquire the temperature distribution by solving the Pennes' bioheat equation [14] as follows:

$$\rho c_\rho \frac{\partial T}{\partial t} = \nabla \cdot (\kappa \nabla T) + \rho \mathrm{SAR} + Q_m - B(T - T_{\mathrm{blood}}) \tag{2}$$

where T is the unknown temperature as a function of time and space, ρ represents the density, c_ρ refers to the specific heat capacity, κ is the thermal conductivity, Q_m denotes the metabolic heat generation, B is related to the blood perfusion, and T_{blood} is the blood temperature.

Solution of (2) requires a predefined boundary condition and an initial condition. Usually, a convection boundary condition is adopted on the skin–air interface

$$-\hat{n} \cdot \kappa \nabla T = h(T - T_{\mathrm{sur}}) \tag{3}$$

where h represents the convective heat transfer coefficient and T_{sur} denotes the surrounding temperature. This boundary condition is utilized to describe the heat exchange between the skin and the air.

As mentioned earlier, all objects that are above absolute zero temperature radiate electromagnetic waves to surroundings. Hence, the radiation phenomenon of skin is also considered by using the radiation boundary condition [15] as follows:

$$-\hat{n} \cdot \kappa \nabla T = \varepsilon_0 \sigma \left(T^4 - T_{\mathrm{sur}}^4\right) \tag{4}$$

where ε_0 refers to the emissivity of the skin and $\sigma = 5.68 \times 10^{-8}$ W/m^{2}K^4 is the Stefan–Boltzmann constant.

The initial condition for the partial differential equation (2) can be specified as

$$T(\mathbf{r}; t = 0) = T^0(\mathbf{r}) \tag{5}$$

where $T^0(\mathbf{r})$ represents the temperature distribution at $t = 0$.

The time-domain FEM (TDFEM) is employed to solve (2) to obtain the time-varying temperature distribution. Tetrahedral elements are adopted to mesh the human head model. The temperature T in each element is expanded by nodal basis functions. Then, the spatially discrete form of (2) can be obtained with the Galerkin's scheme as

$$[C]\left\{\frac{\partial T}{\partial t}\right\} + [K]\{T\} = \{f(T)\} \tag{6}$$

where

$$[C]_{ij} = \rho c_\rho \int_V N_i N_j dV \tag{7}$$

$$[K]_{ij} = \kappa \int_V \nabla N_i \cdot \nabla N_j dV + B \int_V N_i N_j dV + h \int_S N_i N_j dS \tag{8}$$

$$\{f(T)\} = \int_V N_i \rho \mathrm{SAR} dV + \int_V N_i Q_m dV + B \int_V N_i T_{\mathrm{blood}} dV + h \int_S N_i T_{\mathrm{sur}} dS - \varepsilon_0 \sigma \int_S N_i (T^4 - T_{\mathrm{sur}}^4) dS \tag{9}$$

where N_i and N_j denote the ith and jth nodal basis functions, respectively. $\{T\}$ is constituted by the temperature at the nodes of tetrahedral elements.

In order to obtain an unconditionally stable system, the Crank–Nicolson scheme is utilized for the temporal discretization of (6) as

$$\left([C] + [K]\frac{\Delta t}{2}\right)\{T_i\} = \left([C] - [K]\frac{\Delta t}{2}\right)\{T_{i-1}\} + \{f(T_i)\}\Delta t \tag{10}$$

where $\{T_i\}$ contains the temperature of all the nodes at $t_i = i\Delta t$, Δt is the time-step size. Obviously, (10) is nonlinear since the term T_i^4 is included in $\{f(T_i)\}$. A fixed-point iteration method

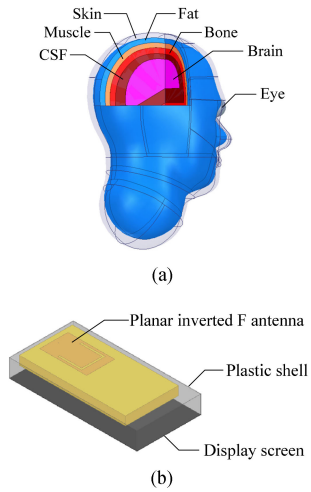

Fig. 2. (a) Head model. (b) Cell phone model.

TABLE I
ELECTROMAGNETIC AND THERMAL PARAMETERS OF HEAD MODEL

Tissues	ε_r	σ	κ	c_ρ	ρ	Q_m	B
Skin	41.4	0.87	0.42	3500	1010	1000	9100
Fat	11.3	0.11	0.25	2500	920	180	520
Muscle	55.0	0.94	0.5	3600	1040	690	2700
Bone	12.5	0.14	0.4	1300	1810	0	1000
CSF	74.0	2.12	0.6	4000	1010	0	0
Brain	45.8	0.77	0.5	3630	1040	10000	35000
Eye	49.6	0.994	0.53	3615	1052	0	0

is used to solve this nonlinear equation as follows:

$$\left([C]+[K]\frac{\Delta t}{2}\right)\left\{T_i^{(n+1)}\right\} = \left([C]-[K]\frac{\Delta t}{2}\right)\{T_{i-1}\}+\left\{f\left(T_i^{(n)}\right)\right\}\Delta t. \quad (11)$$

The initial value of $\{T_i^{(n)}\}$ is set to be $\{T_i^{(0)}\} = \{T_{i-1}\}$ before the iteration process. At the nth iteration, (11) is solved with a multifrontal method for sparse linear equations. The termination criterion for iteration is

$$\left\|\left\{T_i^{(n+1)}\right\}-\left\{T_i^{(n)}\right\}\right\| \le \delta \quad (12)$$

and δ equal to 10^{-3}.

III. NUMERICAL RESULTS

A. Model and Simulation Parameters

Fig. 2(a) shows the head model. It is constituted by skin, fat, muscle, cortical bones, cerebrospinal fluid (CSF), brain, and eyes. The corresponding electromagnetic and thermal parameters are given in Table I.

The cell phone model is shown in Fig. 2(b). It contains a planar inverted-F antenna, a display screen, and a plastic shell. The working frequency of the antenna is 900 MHz. Its input power is 1 W.

All the computations are carried out on a work station with 192 GB RAM and two 2.0 GHz CPUs. Each CPU has eight cores. The parallel computation with 16 cores is adopted for the following simulations.

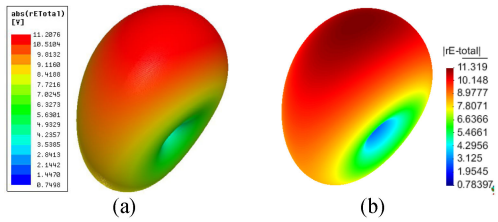

Fig. 3. Radiation pattern obtained by the (a) HFSS software and (b) FE-IIEE method.

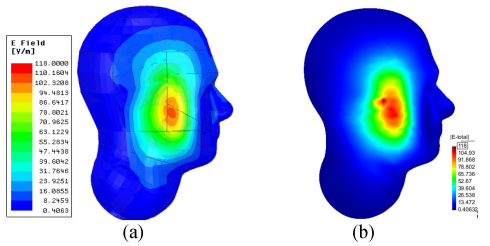

Fig. 4. Electric field amplitudes within the skin layer of the human head model obtained by (a) HFSS software and (b) FE-IIEE method.

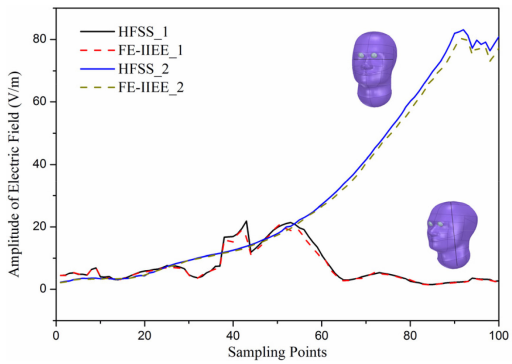

Fig. 5. Electric field amplitudes along two line segments obtained by the HFSS software and the FE-IIEE method. The first line segment is from the center of left ear to the center of right ear. The second line segment is from the center of the neck to the center of the top of the head model.

B. Electromagnetic Simulation

First, the electromagnetic radiation of the cell phone model is simulated by the FE-IIEE method and HFSS software. As the shown in Fig. 3, the radiation pattern obtained by the FE-IIEE method agrees well with the HFSS software.

Second, the human head model is exposed to the radiation of the cell phone with a gap distance of 1 cm. The cell phone is not in contact with the skin. This case is still analyzed by the FE-IIEE method and the HFSS software. The obtained three-dimensional (3-D) electric field amplitudes within the skin layer of the head model are shown in Fig. 4. The electric field amplitudes along two line segments inside the head model are given in Fig. 5. One hundred sampling points are taken along each line. Again, the results of FE-IIEE method and HFSS software agree well with other. The CPU time and memory requirement of the FE-IIEE method are 510 s and 32.5 GB, respectively.

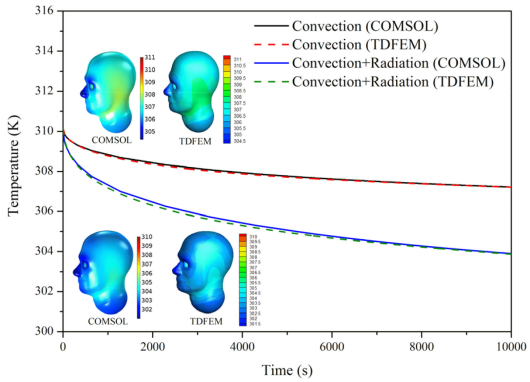

Fig. 6. 3-D temperature distributions at $t = 10\,000$ s and the temporal temperatures at a randomly chosen observation pointobtained by (a) COMSOL software and (b) TDFEM.

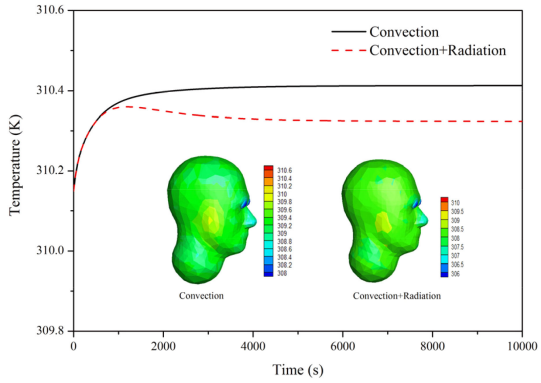

Fig. 7. 3-D temperature distributions at $t = 6000$ s and the temporal temperatures at a randomly chosen observation point obtained by the proposed electromagnetic and thermal cosimulation method.

C. Thermal Simulation

First, an individual thermal simulation is performed, and the result is compared with COMSOL software to validate the TDFEM for thermal simulation. To be consistent with the heat conduction equation utilized in the solid heat transfer module of COMSOL software, ρSAR and B are set to be zero. A uniform volume heat source is assumed and $Q_m = 1000$ W/m^3. The initial temperature of the head model is 37 °C. The room temperature is 25 °C. Fig. 6 shows the results with only the convection boundary condition imposed on the surface of the head model and $h = 5$ W/(m$^2 \cdot$ K), and the results with both the convection and radiation boundary condition imposed and $\varepsilon_0 = 0.95$. The 3-D temperature distributions at $t = 10\,000$ s and the temporal temperatures at a randomly chosen observation point (0.024, −0.024, and 0.021 m) are given. Obviously the results of the TDFEM agree well with the COMSOL software.

Second, the electromagnetic and thermal cosimulation is performed. Using the electric field within the human head model calculated in Section III-B, the SAR distribution can be obtained according to (1). Then, the SAR value is input to the bioheat equation to study the heat transfer within the head model. Again the convection boundary condition with $h = 5$ W/(m$^2 \cdot$ K) and radiation boundary condition with $\varepsilon_0 = 0.95$ are considered. Fig. 7 shows the 3-D temperature distributions at $t = 6000$ s and the temporal temperatures at a randomly chosen observation point (0, −0.026, and 0.043 m) inside the brain. The highest temperature increase with the convection boundary condition is about 0.25 °C, while it is 0.15 °C with both convection and radiation boundary condition. Thus, it is worth mentioning that the temperature will be overestimated if radiative cooling is neglected. The CPU time and memory requirement for thermal simulation are 61 s and 56 MB, respectively.

IV. Conclusion

The electromagnetic and thermal cosimulation of a human head model exposed to cell phones based on the FEM is studied in this letter. Both the convective and radiative boundary conditions are adopted during the thermal simulation stage. Numerical examples validate the correctness of the proposed method. Moreover, it is found that the radiative cooling phenomenon cannot be neglected if a highly accurate temperature distribution is expected.

References

[1] A. C. Guyton and J. E. Hall, *Textbook of Medical Physiology*. Philadelphia, PA, USA: Saunders, 1996.

[2] H. R. Chuang, "Human operator coupling effects on radiation characteristics of a portable communication dipole antenna," *IEEE Trans. Antennas Propag.*, vol. 42, no. 4, pp. 556–560, Apr. 1994.

[3] Y. P. Chen, S. Sun, L. L. Jiang, and W. C. Chew, "A calderón preconditioner for the electric field integral equation with layered medium Green's function," *IEEE Trans. Antennas Propag.*, vol. 62, no. 4, pp. 2022–2030, Apr. 2014.

[4] P. Bernardi, M. Cavagnaro, S. Pisa, and E. Piuzzi, "Specific absorption rate and temperature increases in the head of a cellular-phone user," *IEEE Trans. Microw. Theory Techn.*, vol. 48, no. 7, pp. 1118–1126, Jul. 2000.

[5] P. Bernardi, M. Cavagnaro, S. Pisa, and E. Piuzzi, "Power absorption and temperature elevations induced in the human head by a dual-band monopole-helix antenna phone," *IEEE Trans. Microw. Theory Techn.*, vol. 49, no. 12, pp. 2539–2546, Dec. 2001.

[6] P. A. Mason *et al.*, "Effects of frequency, permittivity, and voxel size on predicted specific absorption rate values in biological tissue during electromagnetic-field exposure," *IEEE Trans. Microw. Theory Techn.*, vol. 48, no. 11, pp. 2050–2058, Nov. 2000.

[7] K. K. Niu, Z. X. Huang, M. Q. Li, and X. L. Wu, "Optimization of the artificially anisotropic parameters in WCS-FDTD method for reducing numerical dispersion," *IEEE Trans. Antennas Propag.*, vol. 65, no. 12, pp. 7389–7394, Dec. 2017.

[8] T. Togashi *et al.*, "FDTD calculations of specific absorption rate in fetus caused by electromagnetic waves from mobile radio terminal using pregnant woman model," *IEEE Trans. Microw. Theory Techn.*, vol. 56, no. 2, pp. 554–559, Feb. 2008.

[9] S. S. Seker, B. O. Demirbilek, and A. Morgul, "SAR assessment in a human head model exposed to radiation from mobile phone using FEM," in *Proc. Int. Symp. IEEE Electromagn. Compat.*, Minneapolis, MN, USA, 2002, vol. 2, pp. 662–666.

[10] T. Wessapan, S. Srisawatdhisukul, and P. Rattanadecho, "Specific absorption rate and temperature distributions in human head subjected to mobile phone radiation at different frequencies," *Int. J. Heat Mass Transf.*, vol. 55, pp. 347–359, 2012.

[11] R. S. Chen, L. Du, Z. Ye, and Y. Yang, "An efficient algorithm for implementing the Crank–Nicolson scheme in the mixed finite-element time-domain method," *IEEE Trans. Antennas Propag.*, vol. 57, no. 10, pp. 3216–3222, Oct. 2009.

[12] M. Salazar-Palma, T. K. Sarkar, L. E. Garc´ıa-Castillo, T. Roy, and A. R. Djordjevic, *Iterative and Self-Adaptive Finite-Elements in Electromagnetic Modeling*. Norwood, MA, USA: Artech House, 1998.

[13] D. Garcia-Donoro, A. Amor-Martin, L. E. Garcia-Castillo, M. Salazar-Palma, and T. K. Sarkar, "HOFEM: Higher order finite element method simulator for antenna analysis," in *Proc. Int. Conf. IEEE Antenna Meas. Appl.*, Syracuse, NY, USA, 2016, pp. 1–4.

[14] H. H. Pennes, "Analysis of tissue and arterial blood temperatures in the resting human forearm," *J. Appl. Phys.*, vol. 85, no. 1, pp. 5–34, Jul. 1998.

[15] H. H. Zhang, W. E. I. Sha, Z. X. Huang, and G. M. Shi, "Flexible and accurate simulation of radiation cooling with FETD method," *Sci. Rep.*, vol. 8, no. 1, pp. 2652–2661, Feb. 2018.